

Synthesis and properties of substituted ferrite-garnet films for one-dimensional magnetophotonic crystals

*V.N.Berzhansky, A.V.Karavainikov, E.T.Milyukova,
T.V.Mikhailova, A.R.Prokopov, A.N.Shaposhnikov*

V.Vernadsky National Taurida University,
4 V.Vernadsky Ave., Simferopol 95007, Ukraine

Received December 23, 2009

Using various deposition and crystallization techniques, substituted ferrite-garnet films of general formula $Y_{3-x-y}Bi_xR_yFe_{5-z}M_zO_{12}$ (R — Gd, Lu; M — Ga, Al), including the compositions having the compensation temperatures exceeding room one has been synthesized. Studied has been the effect of the target composition, deposition and annealing conditions on the crystallization process, the film composition, surface morphology, optical and magneto-optical properties. The magnetic compensation temperatures of the films have been measured, the compensation temperature as a function of the target composition and annealing temperature has been studied. The optimum synthesis conditions have been determined for the films having rather high values of the Faraday rotation angle and the transmission coefficient as well as for those having rather high squareness ratio of the hysteresis loop. The formed films can be used as magnetic layers in magnetophotonic crystals while the latter ones, in the magneto-optical recording devices.

С использованием различных методов напыления и способов кристаллизации были получены пленки замещенных феррит-гранатов общей формулы $Y_{3-x-y}Bi_xR_yFe_{5-z}M_zO_{12}$ (R — Gd, Lu; M — Ga, Al), в том числе составов с температурой компенсации выше комнатной. Исследовано влияние состава мишени, условий напыления и отжига на процесс кристаллизации, состав, морфологию поверхности, оптические и магнитооптические свойства пленок. Проведены измерения температуры магнитной компенсации пленок, исследована зависимость температуры компенсации от состава мишени и температуры отжига. Определены оптимальные режимы синтеза пленок с достаточно высокими значениями угла фарадеевского вращения и коэффициента пропускания, а также пленок с достаточно высоким коэффициентом прямоугольности петли гистерезиса. Первые могут быть использованы в качестве магнитных слоев в магнитофотонных кристаллах, вторые — в устройствах магнитооптической записи.

1. Introduction

Substituted ferrite-garnet materials combining high Faraday rotation angle and low absorption in visible and infrared spectral regions are used as magnetic layers for one-dimensional magnetophotonic crystals (1D-MPC). These requirements are obligatory at the 1D-MPC synthesis, because its magneto-optical and optical parameters depend substantially on the properties of the con-

stituting layers [1–4]. Magneto-optical layers of substituted ferrite-garnets of compensational compositions offer an additional opportunity to control the parameters of the 1D-MPC based devices. This work is aimed at synthesis and investigation of magnetic properties of substituted ferrite-garnet films with compositions described by general formula $Y_{3-x-y}Bi_xR_yFe_{5-z}M_zO_{12}$ (R — Gd, Lu; M — Ga, Al), including compositions with compensation temperature T_{comp} above room temperature.

2. Experimental equipment and procedures

The substituted ferrite-garnets magneto-optical layers were synthesized using the reactive ion beam sputtering (RIBS) and diode radio frequency sputtering (DRFS). The targets of the following compositions were used for magneto-optical layers sputtering:

- No.1 — $\text{Bi}_{2.5}\text{Y}_{0.5}\text{Fe}_5\text{O}_{12}$;
- No.2 — $\text{Bi}_{2.5}\text{Gd}_{0.5}\text{Fe}_{3.8}\text{Al}_{1.2}\text{O}_{12}$;
- No.3 — $\text{Bi}_{1.5}\text{Gd}_{1.5}\text{Fe}_{4.5}\text{Ga}_{0.5}\text{O}_{12}$;
- No.4 — $\text{Bi}_{0.9}\text{Gd}_{1.4}\text{Lu}_{0.7}\text{Fe}_{4.1}\text{Al}_{0.9}\text{O}_{12}$;
- No.5 — $\text{Bi}_{1.5}\text{Gd}_{1.5}\text{Fe}_{4.5}\text{Al}_{0.5}\text{O}_{12}$.

The selection of target chemical compositions was determined by the need for optimization of films characteristics such as the Faraday rotation angle value θ_F , saturation magnetization, coercive force H_c , compensation temperature T_{comp} and Curie temperature T_C , transmittance K_t , squareness ratio of magneto-optical Faraday hysteresis loops (FHLs) K_S . The targets were prepared by conventional ceramic technique [5] in several stages: (i) cold pressing of homogenized mixtures at the pressure of 300 kg/cm²; (ii) first solid-phase synthesis in air at atmosphere pressure and temperature 900°C for 8 hours; (iii) grinding, repeated homogenization and cold pressing of mixtures; and (iv) second solid-phase synthesis at the same conditions. According to X-ray phase analysis, two phases of $\text{Bi}_2\text{Fe}_4\text{O}_9$ and BiFeO_3 are the main constituents of target No.1 after second solid-phase synthesis, mass fractions of the phases were 22 % and 78 %, respectively. In others targets, little shift of those phase peaks as compared to the target No.1 evidenced the presence phases comprising Gd, Lu, Al.

Single crystal plates of gadolinium-gallium (GGG) and calcium-niobium-gallium (CNGG) garnets with lattice parameters $\alpha_{GGG} = 1.2383$ nm and $\alpha_{CNGG} = 1.2507$ nm were used as substrates. The films were crystallized using three different methods: during deposition on hot substrate (*in situ*), annealing in a vacuum chamber in presence of oxygen and air annealing at atmosphere pressure. The synthesis by RIBS method was carried out at ion acceleration voltage $U = 5$ kV and ion beam current $I = 100$ mA. The films were deposited both in pure argon atmosphere and in argon-oxygen mixture at different partial pressures. The film deposition rate on cold substrate was 7–10 nm/min, on hot substrate (*in situ*), 1.5–2.5 nm/min. The an-

nealing duration was varied from 5 to 20 minutes in vacuum chamber and from 0.5 to 15 hours in air. The synthesis by DRFS method was carried out onto a hot substrate at substrate temperature $T_s = 680$ – 700°C in argon or in argon with oxygen addition. The discharge power was varied from 5 to 8 kW. The deposition rate of films synthesized by this method was about 10 nm/min. Optimum regimes of film synthesis using both the methods are presented in Table 1.

The lattice parameters of synthesized films were determined using a DRON-2 diffractometer. The surface state of sputtered films as well as chemical composition of targets and films were determined using a REM-106 raster electronic microscope with energy dispersion spectrometer EDS-1. Thickness h and refractive index n of the films were measured using a Biolar PI polarization-interference microscope by double immersion method. The film magneto-optical characteristics (θ_F , H_c , K_s , T_C , T_{comp}) were determined from FHLs measured by Faraday magnetopolarimeter at 655 nm wavelength in temperature range from 25 to 180°C. K_t was measured by an SP-14 spectrophotometer in wavelength range from 400 to 750 nm.

3. Results and discussion

The films deposited by RIBS method on hold substrates from all types of targets and annealed in air during 0.5–15 hours at temperatures $T_a < 600^\circ\text{C}$ had amorphous structures and did not display magnetic properties at room temperature. The lowest crystallization temperature determined by appearance of FHL was 600°C. The SEM-photographs of film surfaces deposited from target No.2 and annealed at different T_a are presented in Fig. 1. The crystallization extent of films is seen to depend on T_a . The morphology of the film annealed at $T_a = 770^\circ\text{C}$ shows a maximum homogeneity (Fig. 1, c). For that film, maximum θ_F and K_t values are observed. According to the microanalytical data, films with a higher Bi^{3+} ion concentration were obtained at lower T_s and T_a . This is connected with an essential condensation temperature distinction of Bi containing vapors in comparison with other garnet constitutive elements as well as with Bi evaporation during annealing. The amount of regions depleted of Bi (dark dots) and the size of crystallites increases with increasing T_a (to 1 μm at $T_a = 910^\circ\text{C}$). Decay of garnet phase is observed at $T_a > 910^\circ\text{C}$ (Fig. 1, e, f).

Table 1. Optimal regimes of film synthesis

Reactive ion beam sputtering (U = 5 kW, I = 100 mA)				
1. On hot GGG substrate with crystallization <i>in situ</i>				
Synthesis condition	Chemical composition of targets			
	Bi _{2.5} Y _{0.5} Fe ₅ O ₁₂	Bi _{2.5} Gd _{0.5} Fe _{3.8} Al _{1.2} O ₁₂	Bi _{1.5} Gd _{1.5} Fe _{4.5} Ga _{0.5} O ₁₂	Bi _{0.9} Gd _{1.4} Lu _{0.7} Fe _{4.1} Al _{0.9} O ₁₂
P_b , Torr	5·10 ⁻⁶			
P_{Ar} , Torr	5·10 ⁻⁴			
P_{O_2} , Torr	0.5·10 ⁻⁴	0.5·10 ⁻⁴	0.6·10 ⁻⁴	0.6·10 ⁻⁴
T_s , °C	560	560	590	650
2. On cold substrate GGG with crystallization in air				
P_b , Torr	5·10 ⁻⁶			
P_{Ar} , Torr	5·10 ⁻⁴			
T_a , °C (t_a)	600–960 (3 h.)			
3. On cold substrate GGG with crystallization in vacuum chamber				
Synthesis condition	Chemical composition of targets			
	Bi _{1.5} Gd _{1.5} Fe _{3.8} Al _{1.2} O ₁₂		Bi _{2.5} Y _{0.5} Fe ₅ O ₁₂	
P_{O_2} , Torr	0.7			
T_a , °C (t_a)	650 (15 min)		520 (15 min)	
Radiofrequency diode sputtering on hot substrate with crystallization <i>in situ</i>				
Synthesis condition	Chemical composition of targets (substrate)			
	Bi _{1.5} Gd _{1.5} Fe _{4.5} Al _{0.5} O ₁₂ (CNGG)		Bi _{1.5} Gd _{1.5} Fe _{4.5} Al _{0.5} O ₁₂ (GGG)	
T_s , °C	700		680	
P_{Ar} , Torr	6·10 ⁻⁴			
W , kW	8			
P_{O_2} , Torr	1·10 ⁻⁴			

Notation: P_b — background pressure, P_{Ar} — argon pressure, P_{O_2} — oxygen pressure, T_s — substrate temperature, U — accelerated voltage, I — ion beam current, T_a — annealing temperature, t_a — annealing time, W — discharge power.

These processes are reflected in corresponding FHLs that will be showed below.

An interesting peculiarity of crystallization processes in films deposited from targets Nos.2–4 is the inversion of FHLs at T_a exceeding a certain value (Fig. 2, a). For example, samples of films deposited from target No.2 and annealed at $T_a \geq 840^\circ\text{C}$ have the inverse sign of θ_F and "left" FHLs as compared to samples annealed at lower T_a and having "right" FHLs. For these samples, the T_a increasing from 600 to 770°C is accompanied by θ_F increasing from minimum to maximum value. This can evidence both the increasing crystal phase volume in the films and of thermoactivated redistribution of garnet constitutive elements with garnet formation of other composition. In our opinion, the second process is the key

one in connection with decrease of θ_F value and its subsequent inversion at $T_a \geq 840^\circ\text{C}$. The maximum reverse value of θ_F is observed at $T_a = 910^\circ\text{C}$. The θ_F decrease at $T_a = 910^\circ\text{C}$ is due to the garnet phase decay. It is to note that with increasing T_a , K_t decreases from 72 to 47 % at 655 nm wavelength.

The film samples with "left" FHLs are characterized by presence of compensation temperature T_{comp} exceeding room temperature and depending on T_a : T_{comp} increases from 40 to 145°C with T_a increasing from 850 to 910°C.

Fig. 2, b shows the θ_F temperature dependences for samples of the same film with "right" and "left" FHLs. In film annealed at $T_a = 770^\circ\text{C}$, θ_F remains constant up to 90°C and then decreases when temperature

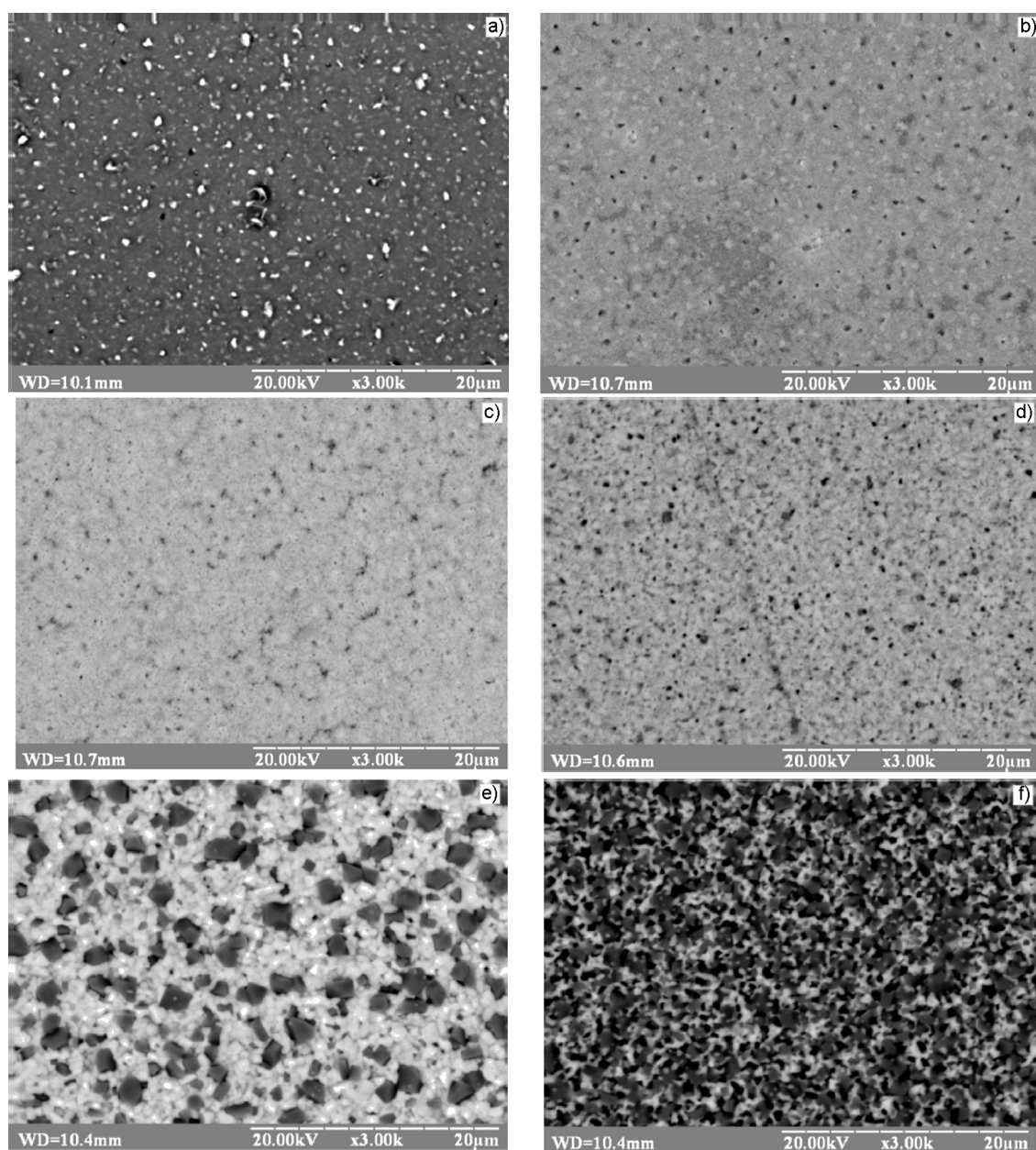


Fig. 1. SEM surface images of film samples deposited from target No.2 and annealed at different temperatures: a) no annealing; b) $T_a = 635^\circ\text{C}$; c) $T_a = 770^\circ\text{C}$; d) $T_a = 850^\circ\text{C}$; e) $T_a = 910^\circ\text{C}$; f) $T_a = 960^\circ\text{C}$.

approaches T_C . In film annealed at $T_a = 850^\circ\text{C}$, θ_F decreases with increasing temperature, when T_{comp} attains 40°C , θ_F changes its sign, attains a maximum at 145°C and decreases tending to T_C as in samples with "right" FHLs.

In [6], the θ_F sign change at increasing T_a in films of compensational compositions is explained by oxidation of Fe^{2+} to Fe^{3+} . However, our film chemical composition data confirm the hypothesis of thermoactivated redistribution of garnet constitutive elements in film during the annealing. An-

nealing of films at $T_a > 770^\circ\text{C}$ results in a substantial reduction of bismuth content and in respectively increasing abundance of other elements, including gadolinium. Increasing of rare-earth ions Gd^{3+} fraction in dodecahedral sites of garnet with increasing T_a results in T_{comp} elevation up to room value, change of θ_F sign and appearance of "left" FHLs. Note that dependences similar to those in Fig. 2 were observed for films deposited from targets No.3 and No.4 only the T_a values at which θ_F sign inverses were changed.

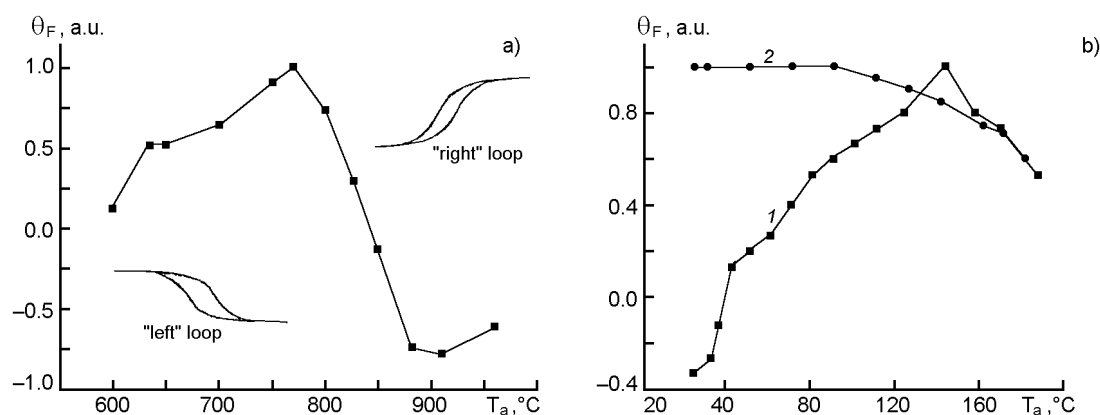


Fig. 2. $\theta_F(T_a)$ dependence for film samples obtained by RIBS from target No.2 (a) and temperature dependences of θ_F for that film samples annealed at $T_a = 770^\circ\text{C}$ (1) and $T_a = 850^\circ\text{C}$ (2) (b).

Table 2. Technical characteristics of synthesized films

Chemical composition of target (substrate)	θ_F , deg/ μm	H_c , Oe	K_t , % $\lambda = 655$ nm	T_C , $^\circ\text{C}$	h , μm
Reactive ion beam sputtering on hot GGG substrate (<i>in situ</i>)					
$\text{Bi}_{2.5}\text{Y}_{0.5}\text{Fe}_5\text{O}_{12}$	-2.2	264	78	>180	0.30
$\text{Bi}_{2.5}\text{Gd}_{0.5}\text{Fe}_{3.8}\text{Al}_{1.2}\text{O}_{12}$	-1.8	239	78	>180	0.41
$\text{Bi}_{1.5}\text{Gd}_{1.5}\text{Fe}_{4.5}\text{Ga}_{0.5}\text{O}_{12}$	-1.3	176	79	180	0.35
$\text{Bi}_{0.9}\text{Gd}_{1.4}\text{Lu}_{0.7}\text{Fe}_{4.1}\text{Al}_{0.9}\text{O}_{12}$	-0.8	151	81	150	0.38
on cold GGG substrate with annealing on air					
$\text{Bi}_{2.5}\text{Y}_{0.5}\text{Fe}_{50}12$	-2.0	189	78	>180	1.2
$\text{Bi}_{2.5}\text{Gd}_{0.5}\text{Fe}_{3.8}\text{Al}_{1.2}\text{O}_{12}$	-1.9	289	58	>180	0.7
$\text{Bi}_{1.5}\text{Gd}_{1.5}\text{Fe}_{4.5}\text{Ga}_{0.5}\text{O}_{12}$	-1.5	339	55	180	1.0
$\text{Bi}_{0.9}\text{Gd}_{1.4}\text{Lu}_{0.7}\text{Fe}_{4.1}\text{Al}_{0.9}\text{O}_{12}$	-0.8	377	53	150	0.8
on cold GGG substrate with annealing in chamber					
$\text{Bi}_{1.5}\text{Gd}_{1.5}\text{Fe}_{4.5}\text{Al}_{0.5}\text{O}_{12}$	1.9	206	82	–	0.9
$\text{Bi}_{2.5}\text{Y}_{0.5}\text{Fe}_5\text{O}_{12}$	3.2	194	80	–	0.3
Diode radiofrequency sputtering on hot substrate (<i>in situ</i>)					
$\text{Bi}_{1.5}\text{Gd}_{1.5}\text{Fe}_{4.5}\text{Al}_{0.5}\text{O}_{12}$ (CNGG)	0.4	656	81	–	0.7
$\text{Bi}_{1.5}\text{Gd}_{1.5}\text{Fe}_{4.5}\text{Al}_{0.5}\text{O}_{12}$ (GGG)	0.75	635	82	–	0.6

As we determined, the best characteristics (sets of parameters) have the films synthesized by RIBS from targets No.1 and No.2 with crystallization *in situ* and with crystallization in vacuum (Table 2). The FHLs for films crystallized by annealing in chamber are presented in Fig. 4. Maximum values of θ_F and K_t are 3.2 and 1.9 deg/ μm , 80 and 82 %, respectively (see Table 2). The H_c for those films are high enough that also evidence their polycrystallinity and high stresses therein. The slope of FHLs

evidences the presence of magnetization vector plane component. The FHLs smoothness and linearity evidence a rather high homogeneity of the films.

Films of $\text{Bi}_{1.5}\text{Gd}_{1.5}\text{Fe}_{4.5}\text{Al}_{0.5}\text{O}_{12}$ composition (target No. 5) were obtained by DRFS. The crystallization was carried out *in situ* during the deposition onto hot GGG and CNGG substrates. The FHLs of those films are shown in Fig. 5. The film on CNGG is characterized by "left" FHL, that on GGG, by "right" FHL. That testifies for the formation of garnets with different composi-

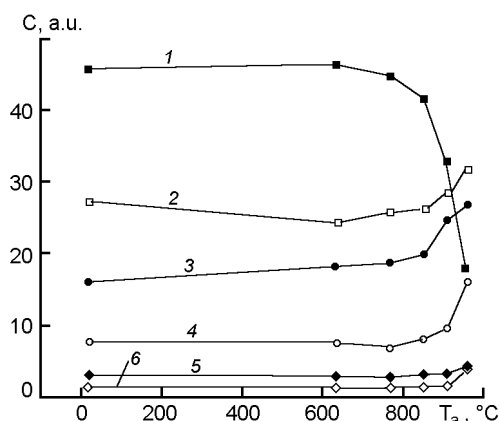


Fig. 3. Dependences element content on T_a in film obtained by RIBS from target No. 2.

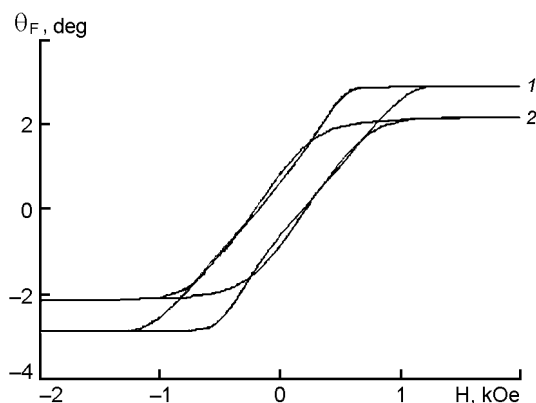


Fig. 4. FHLs of films deposited from targets No. 1 (1) and No. 2 (2) by RIBS on cold substrate with crystallization by annealing in chamber.

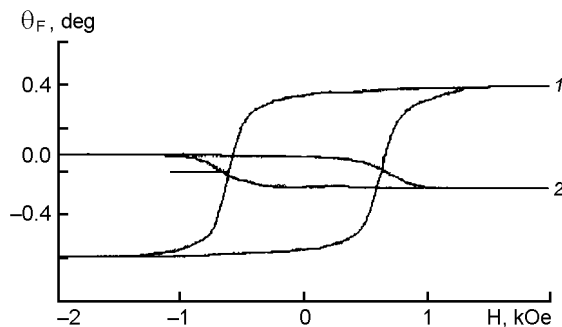


Fig. 5. FHLs of films obtained on GGG (1) and CNGG (2) substrates by DRFS of target No. 5.

tion on these substrates. The films are characterized by high value of FHL squareness

ratio K_s amounting 0.89 and 0.84 for films on GGG and CNGG, respectively. Such high K_s values were not obtained for films deposited by other methods. Perhaps this is a consequence of high uniaxial anisotropy that is characteristic for films obtained by that method [6, 7]. The transmittance for these films at $\lambda = 655$ nm is 82 and 81 %, respectively.

4. Conclusions

Using reactive ion beam and diode radio frequency sputtering and different crystallization techniques, the films of substituted ferrite-garnets of general formula $Y_{3-x-y}B_{ix}R_yFe_{5-z}M_zO_{12}$ (where R — Gd, Lu; M — Ga, Al), have been synthesized, including the films with compensation temperature above room temperature. Dependence of compensation temperature on the annealing temperature has been established for films of compensational compositions. This is connected with thermoactivated redistribution of garnet constitutive elements and formation of garnet with different composition. The best magneto-optical characteristics ($\theta_{Fmax} = 3.20$ deg/ μm , $K_t = 80$ %) show the films synthesized by RIBS with crystallization by annealing in vacuum chamber in the presence of oxygen which can be used in 1D-MPC based devices. The films with high FHL squareness ratio have been obtained by radio frequency diode sputtering method. Such films can be used in devices for thermomagnetic data recording.

References

1. P.Johansson, S.I.Khartsev, A.M.Grishin, *Thin Solid Films*, **515**, 477 (2006).
2. S.Kahl, Dr. Sci. Thesis: Condensed Matter Physics, Royal Institute of Technology (2004), p.133.
3. I.L.Lyubchanskii, N.N.Dadoenkova, M.I.Lyubchanskii et al., *J. Phys. D*, **36**, R277 (2003).
4. M.Inoue, H.Uchida, K.Nishimura, P.B.Lim, *J. Mater. Chem.*, **16**, 678, (2006).
5. T.Okuda et al., *IEEE Trans. J. Magn. Jap.*, **23**, 3491 (1987).
6. M.Gomi, K.Utsugi, M.Abe, *IEEE Trans. Magn.*, **22**, 1233 (1986).
7. M.Gomi, T.Tanida, M.Abe, *J. Appl. Phys.*, **57**, 3888 (1985).

Синтез та властивості плівок заміщених ферит-гранатів для одновимірних магнітофотонних кристалів

***В.Н.Бержанський, А.В.Каравайніков, О.Т.Мілюкова,
Т.В.Михайлова, А.Р.Прокопов, О.М.Шапошніков***

З використанням різних методів напилення та способів кристалізації отримано плівки заміщених ферит-гранатів загальної формули $Y_{3-x-y}Bi_xR_yFe_{5-z}M_zO_{12}$ (R — Gd, Lu; M — Ga, Al), у тому числі складів з температурою компенсації вище кімнатної. Досліджено вплив складу мішені, умов напилення і відпалу на процес кристалізації, склад, морфологію поверхні, оптичні та магнітооптичні властивості плівок. Проведено вимірювання температури магнітної компенсації плівок, досліджено залежність температури компенсації від складу мішені і температури відпалу. Визначено оптимальні режими синтезу плівок з досить високими значеннями кута фарадеївського обертання і коефіцієнта пропускання, а також плівок з досить високим коефіцієнтом прямокутності петлі гістерезису. Перші можуть бути використані як магнітні шари у магнітофотонних кристалах, другі — у пристроях магнітооптичного запису.